Radiation Measurements 133 (2020) 106294

Contents lists available at ScienceDirect

Radiation Measurements

journal homepage: http://www.elsevier.com/locate/radmeas

Monte Carlo simulation of the CERN-EU High Energy Reference Field (CERF) facility

T. Brall [a,*], M. Dommert [b], W. Rühm [a], S. Trinkl [c], M. Wielunski [a], V. Mares [a]

[a] Helmholtz Zentrum München, Institute of Radiation Medicine, Ingolstädter Landstraße 1, D-85764, Neuherberg, Germany
[b] Physikalisch-Technische Bundesanstalt, Bundesallee 100, 38116, Braunschweig, Germany
[c] Federal Office for Radiation Protection (BFS), Ingolstädter Landstraße 1, 85764, Neuherberg, Germany

ARTICLE INFO

Keywords:
CERF
Monte Carlo simulation
Geant4
FLUKA
Bonner sphere spectroscopy
High-energy neutrons

ABSTRACT

In the present paper Geant4 Monte Carlo simulations of the CERN-EU high-energy Reference Field (CERF) facility in Geneva, Switzerland, are presented. At this facility a neutron field with a broad energy distribution from thermal energies up to GeV is available. To validate the simulated neutron fluences, the CERF neutron energy distribution was also measured with an extended range Bonner Sphere Spectrometer. Both measurements and simulations are compared against the official CERF reference distributions that were calculated with the Monte Carlo code FLUKA. It turned out that the differences between the total neutron fluences simulated with Geant4 and those measured were less than 41%, depending on the measurement position. While the total fluences simulated with the Geant4 Binary INC model (QGSP_BIC_HP) and the corresponding FLUKA reference values were up to 41% lower than those measured, the total fluences simulated with the Geant4 Bertini INC model (QGSP_BERT_HP) overestimated (up to 27%) the experimental results. As compared to the measured ambient dose equivalent H*(10), similar differences were observed with H*(10) values higher by about 29% for the Geant4 Bertini INC simulations and lower by about 48% for the Geant4 Binary INC and FLUKA simulations.

1. Introduction

Neutrons with energies above 20 MeV (called "high-energy neutrons" hereafter) represent an essential component of secondary particles produced at particle accelerators used for example in hadron therapy facilities and elementary particle research centers. Furthermore, they are produced in nature through the interaction of primary cosmic radiation particles (mainly protons) with the nuclei of the Earth's atmosphere. Although this is known since many decades, it is still challenging to quantitatively detect and simulate high-energy neutron fields at various applications. This is so because experimental data of nuclear interaction cross section are still scarce for high-energy neutrons. To study the physics of high-energy interactions, which is important for example for dosimetry, radiation protection monitoring of workplaces, and radiation effects in electronics, well-characterized high-energy neutron fields are needed, but only a few exist world-wide (Schuhmacher, 2004; Pomp et al., 2013; Alves et al., 2015).

In 1992, supported by the Coordinating European Council (CEC), the European Organization for Nuclear Research (Conseil Européen pour la Recherche Nucléaire - CERN) has provided a CERN-EU High-Energy Reference Field (CERF) facility at the Super Proton Synchrotron (SPS) which simulates the radiation fields at commercial flight altitudes and around high energy hadron accelerators (Aroua et al., 1994; Höfert and Stevenson, 1994; Schraube et al., 1999).

These radiation environments are dominated by neutrons with energy ranging from thermal energies up to several GeV, but other components of the radiation field (mainly photons) are also present. Since 1993, CERF is for example used for testing and calibrating active and passive radiation dosemeters for radiation protection applications in aviation, space, and at particle accelerator facilities (see e.g. Mares et al., 1998; Mitaroff and Silari, 2002; Silari and Pozzi, 2017; Wielunski et al., 2018; Dinar et al., 2018).

Because measurement of the energy distributions of those various particles in such a mixed radiation field is very complex, the particle spectral fluences at each CERF calibration position were obtained by Monte Carlo (MC) radiation transport simulations. Initially, these simulations were done using the MC code FLUKA (Fasso et al., 1993). More details on the CERF reference data obtained in such a way are given in Birattari et al. (1998). It should be noted, however, that these data were calculated more than 20 years ago using the FLUKA92 version and a

* Corresponding author.
E-mail address: tbrall@gmx.de (T. Brall).

https://doi.org/10.1016/j.radmeas.2020.106294
Received 6 August 2019; Received in revised form 31 January 2020; Accepted 27 February 2020
Available online 6 March 2020

rather simplified geometric model of the CERF facility (Silari and Pozzi, 2017). First GEANT4 simulations of the facility and comparison with previously published FLUKA data was performed by Prokopovich et al. (2010). In the present study GEANT4 (Agostinelli, 2003) (version 10.01 patch 2) is used. In an earlier paper (Wielunski et al., 2018), neutron doses at various reference points on top of the concrete and iron shielding of the CERF facility were measured by means of an in-house electronic neutron dosemeter (Wielunski et al., 2018, 2004), and compared to those provided by the CERF facility (http://tis-div-rp-cerf.web.cern.ch/tis-div-rp-cerf). While the earlier paper compared measured neutron doses and neutron energy distributions with those obtained with FLUKA reference simulations, the present paper describes, for the same experiment, the results of a concomitant study which focusses on simulation of neutron spectra at various CERF reference positions using the GEANT4 code and comparison to the earlier FLUKA reference neutron energy spectra (http://tis-div-rp-cerf.web.cern.ch/tis-div-rp-cerf).

The aim of the present study was to compare GEANT4 and earlier FLUKA reference simulations with experimental measurements done with an Extended Range Bonner Sphere Spectrometer (ERBSS) and discuss the reliability of the MC models.

2. Materials and methods

2.1. CERN-EU High-Energy Reference Field (CERF) – facility

The CERN-EU High-Energy Reference Field (CERF) is installed in a secondary beam line (H6) of the Super Proton Synchrotron (SPS) at the CERN Prévessin site. There the stray radiation fields are created by a hadron beam with a momentum of 120 GeV/c (or earlier 205 GeV/c) impinging on a 50 cm long copper target (7 cm in diameter) surrounded by a massive concrete and iron shielding. The calibration positions are located outside the shielding. The roof shields of concrete and iron, respectively, produce almost uniform fields of secondary radiation over an area of 2×2 m^2; This area is divided into 16 squares of 50 cm by 50 cm each. The reference measurement positions are at the centre of a 50 x 50×50 cm^3 cube above each square (Fig. 1).

Additional eight measurement positions (in a 2 x 4 grid of 50 cm by 50 cm squares) are located behind the lateral shielding. The CERF facility has already been described in more detail in various publications (Höfert and Stevenson, 1994; Birattari et al., 1998; Mitaroff and Silari, 2002; Nakao et al., 2006).

2.2. GEANT4 Monte Carlo simulation

In the present study, a high-energy particle beam consisting of pions, protons and kaons with a momentum of 120 GeV/c hit a copper target. This beam and the resulting secondary particles were simulated with MC codes and measured at various reference positions (Fig. 1) behind 80 cm thick concrete (walls and roof) and 40 cm thick iron (roof). For this study the MC toolkit GEANT4 was used (Agostinelli, 2003). The simulations were done two different physics lists - "QGSP_BERT_HP" and "QGSP_BIC_HP". Both are reference physics lists of the Geant4 toolkit and both use the high precision neutron model (_HP) for neutrons below 20 MeV, based on the G4NDL cross section library. One main difference of the two physics lists is the hadronic inelastic model for neutrons and protons between 0 and 9.9 GeV were the QGSP_BIC_HP use the Binary cascade and the QGSP_BERT_HP use the Bertini intranuclear cascade. More details about this physics lists are given in the Geant4 Guide for Physics Lists. (Geant4 Collaboration, 2017). The geometry of the CERF facility as implemented in GEANT4 in the present paper is shown in Fig. 2.

The total volume for the simulation geometry was a segment of the facility of 20 x 15 $\times$ 12 m^3. And the dimensions of the geometry were taken from Nakao et al. (2008) and Mitaroff and Silari (2002)). The concrete used in the simulation was ("G4_CONCRETE"), from the Geant4 material database (Geant4 Collaboration, 2014), the composition is listed in (Table 1), while the composition of the iron roof shield was considered to be S235 iron ($\rho = 7.2$ g/cm^3) for the lower part (first 20 cm thick slab) and GG20 iron ($\rho = 7.65$ g/cm^3) for the upper part (second 20 cm thick slab). The iron composition is listed in Agosteo et al. (2013). For each simulation two million primary pions (π^+), one million primary protons (p^+) and primary 200,000 kaons (K^+) were considered with 120 GeV/c, and the resulting neutron spectra were normalized to one primary particle weighted with 65% π^+, 31% p^+ and 4% K^+. This primary particle composition was taken from Mitaroff and Silari (2002). As scoring region a spherical volume of 12.7 cm in diameter was assumed and the Path-Length Estimator was taken to calculate the neutron fluence.

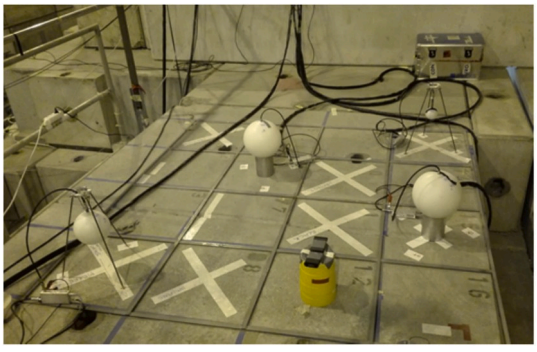

Fig. 1. The CERN-EU High-Energy Reference Field (CERF) facility for dosimetry at commercial flight altitudes and in space. Top of concrete shielding, with four spheres of the Extended Range Bonner Sphere Spectrometer visible.

2.3. Measurement setup

The neutron spectrometer used in this experiment is based on the initial standard Bonner sphere spectrometer (BSS) which was first introduced in 1960 by Bramblett, Ewing and Bonner (Bramblett et al., 1960) but has been much improved. The Extended Range BSS (ERBSS) used in the present study consisted of 15 polyethylene (PE) spheres of different sizes (diameters: 2.5, 3, 3.5, 4, 4.5, 5, 5.5, 6, 7, 8, 9, 10, 11, 12, 15 inch) and four spherical proportional counters filled with ^{3}He gas of 172 kPa partial pressure (type SP9, Centronic Ltd.) which can be placed in the center of each PE sphere. Two further 9 inch PE spheres include additional lead shells (thickness: 0.5 and 1 inch) were used to extend the sensitivity of these spheres to high energies by allowing for Pb(n,xn) reactions induced by the high-energy neutrons (Mares and Schraube, 1998b). Additionally, one ^{3}He proportional counter without any surrounding material ("bare detector") was used to measure thermal neutrons. The electronic system used allowed simultaneous measurement with four spheres.

Unfolding was done with an in-house version of the MSANDB code (Matzke, 1987). MSANDB uses the MC calculated response functions for all channels of the ERBSS, and an initial guess spectrum that includes a-priory physical information on the neutron energy spectrum at the measurement location. This initial neutron energy spectrum is iteratively adjusted by the code to finally match the measured ERBSS count rates. In that procedure, the relative uncertainties associated with the detector counts are used as weighting factors. For the guess neutron energy spectrum needed for initiation of the unfolding procedure (Simmer et al., 2010), the neutron spectra simulated with Geant4 for the corresponding measurement position were taken, as well as the corresponding re-binned CERF reference spectra. The response matrix of the ERBSS (i.e., the response of the 18 Bonner Spheres as a function of neutron energy) was calculated with MCNPX, MCNP and LAHET (Mares et al., 2002, 1998; Mares and Schraube, 1998b). Below 20 MeV, experimental validation of the response functions is described in Alevra

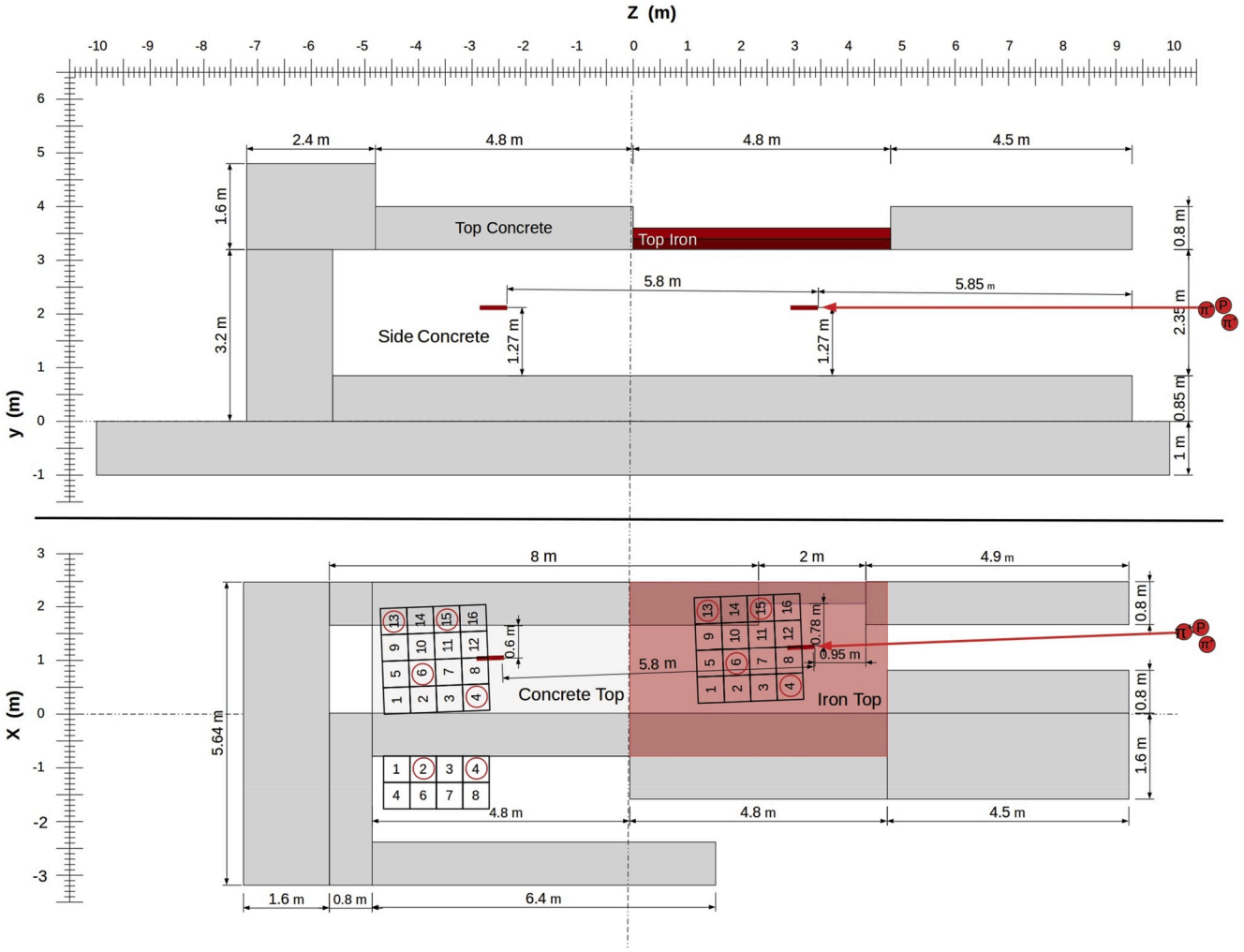

Fig. 2. Detail of the simulated geometry of the CERN-EU High-Energy Reference Field (CERF) facility. Concrete elements are gray, iron top shielding is red. The reference grid is 2 × 2 m^2 on the top positions (2 × 1 m^2 on side concrete), 0.5 × 0.5 m^2 for each reference position. The positions measured and simulated for this work are marked in red. The dimensions were taken from Nakao et al. (2008) and Mitaroff and Silari (2002). (For interpretation of the references to colour in this figure legend, the reader is referred to the Web version of this article.)

Table 1
Composition of the Concrete used in the Simulation with a density of 2.3 g/cm^3. Data were taken from the Geant4 Material Database (Geant4 Collaboration, 2014).

Element	Mass fraction
H	0.01
C	0.001
O	0.529107
Na	0.016
Mg	0.002
Al	0.033872
Si	0.337021
K	0.013
Ca	0.044
Fe	0.014

et al. (1992) and Thomas et al. (1994), while for neutron energies above 20 MeV validation is described in Mares et al., (2013). Fig. 3 shows the response function of the ERBSS.

Spheres of the ERBSS were installed consecutively at the reference positions 4, 6, 13 and 15 on the iron (top of iron - TI) and concrete tops (top of concrete - TC), respectively, and at reference positions 2 and 4 on concrete side walls (side of concrete - SC) (see Fig. 1). The distance of the Bonner sphere center to the top or wall surface was 25 cm. During the measurements the beam intensity was monitored with a high precision ionization chamber (PIC). One Count of this PIC "PIC-cnt" is equivalent to 22,000 primary particles (within ± 10%) (Ferrari et al., 2014).

2.4. CERF reference spectra

CERF provides neutron reference spectra (http://tis-div-rp-cerf.web.cern.ch/tis-div-rp-cerf), calculated with the MC Code FLUKA (Fasso et al., 1993). These FLUKA spectra were re-binned to match the GEANT4 bin-structure (ten bins per decade). Since the FLUKA spectrum has only one bin for energies less than 0.4 eV, for the unfolding guess spectrum at this energy range a Maxwell-Boltzmann distribution was assumed.

3. Results

3.1. GEANT4 simulated neutron energy spectra

GEANT4 neutron energy spectra were calculated for four reference positions on top of the concrete roof (pos. 4, 6, 13, 15), two reference positions at the side wall of the concrete shielding (pos. 2, and 4), and four reference positions on top of the iron roof (pos. 4, 6, 13, 15). Fig. 3 gives, as an example, the resulting GEANT4 neutron energy spectra for

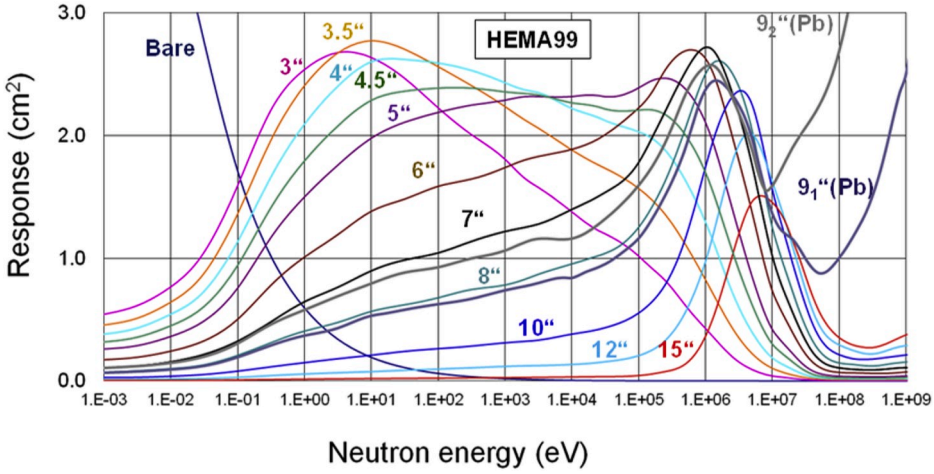

Fig. 3. Response functions of HMGU ERBSS calculated by Monte Carlo simulations as a function of neutron energy (Mares et al., 1991, Mares and Schraube, 1998b).

concrete roof, position 6, in comparison to the corresponding rebinned FLUKA reference spectrum (note that in the low-energy part below 0.4 eV is not presented in this Figure, because the original data have only one bin in this energy region). All results shown in Figs. 4 and 5 are normalized to one primary event.

In this case, the GEANT4 neutron energy spectrum simulated with the Bertini physics list gave the highest values, for the whole energy range. In contrast, the GEANT4 neutron energy spectrum with the Binary physics list is lower and closer to the FLUKA reference spectrum. Note that at thermal energies the local surroundings (e.g., room geometry, room walls) are important which were different in the GEANT4 and FLUKA simulations. Therefore, differences in this energy range are not surprising.

For comparison, Fig. 5 shows the results obtained for position 6 on the iron roof.

In this case, the results obtained using the Bertini and Binary physics lists are closer together, although the Bertini results still seem somewhat higher. As for the concrete roof, the FLUKA reference spectrum seems somewhat lower in most energy bins. These differences can be probable explained by the different composition of iron shielding used in the GEANT4 and FLUKA simulations.

Results obtained for all reference positions are shown in the Appendix (Fig. A1, A2 and A3) and in Table A1. In general, the GEANT4 neutron energy spectra with the Bertini physics list are the highest, in most cases.

In addition, simulated neutron energy spectra appear to be higher at energies >20 MeV than those measured, especially for top concrete, but not for side concrete. The measurements at SC were done with only six of eighteen spheres and we can indeed not rule out that the reduced number of spheres used at this position may have some consequences for the deducted neutron energy distribution. The reason for the experimental ERBSS results to be lower for top concrete than those simulated might be due to the fact that the geometry used in the simulation was different than the geometry present during the measurements.

3.2. ERBSS measured neutron energy spectra

Because it is currently not clear which GEANT4 physics list to be used, an attempt was made to validate those spectra by means of measured ERBSS neutron energy spectra. Figs. 5 and 6 show the neutron energy spectra as measured with the ERBSS at position 6 on the concrete roof (TC06), and at position 6 on the iron roof (TI06), respectively. As starting guess spectra for the unfolding procedure, the simulated neutron energy spectra shown in Figs. 4 and 5 were used. Corresponding

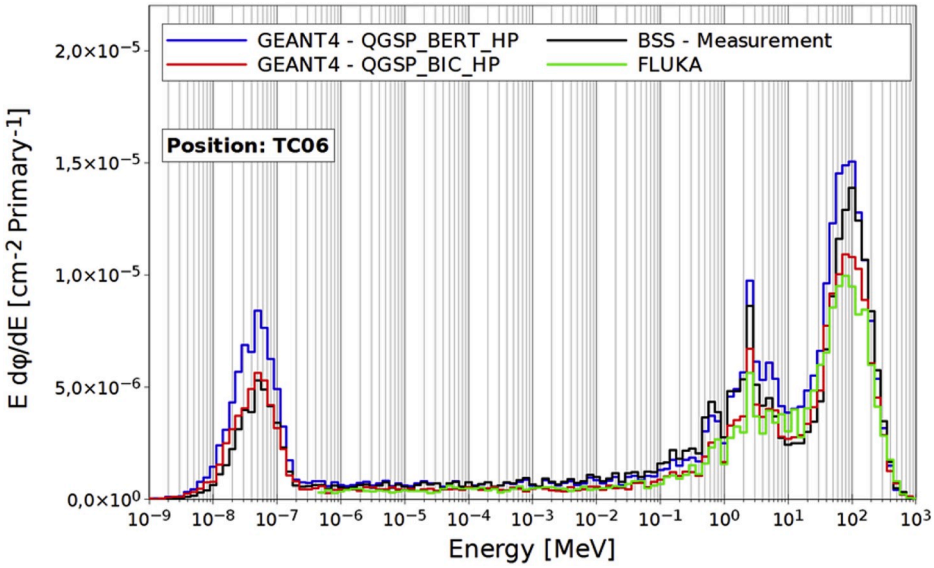

Fig. 4. Neutron energy spectra for pos. 6 on top of the concrete roof (TC06), simulated with GEANT4 (two physics lists) and compared to the re-binned FLUKA reference spectrum (http://tis-div-rp-cerf.web.cern.ch/tis-div-rp-cerf).

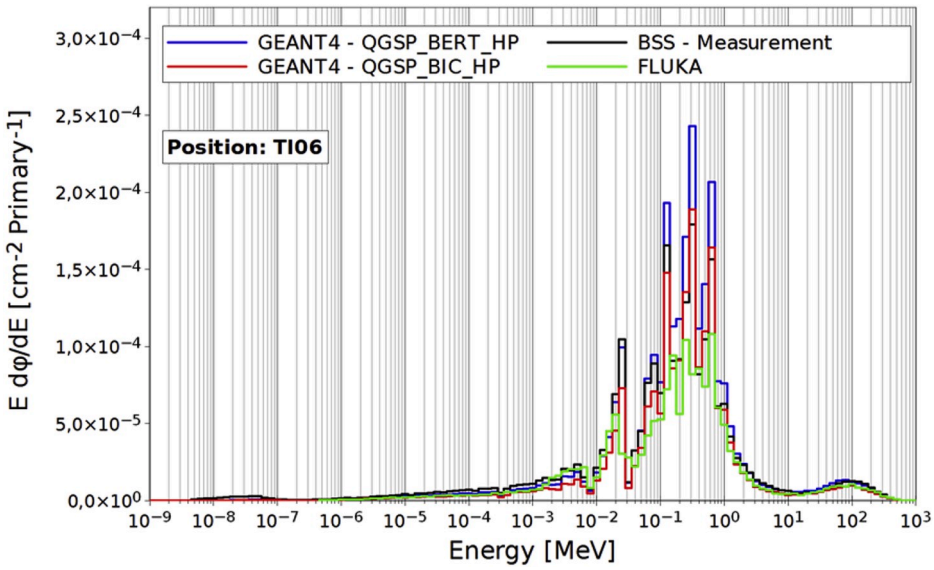

Fig. 5. Neutron energy spectra for pos. 6 on top of the iron roof (TI06) simulated with GEANT4 (two physics lists), and compared to the re-binned FLUKA reference spectrum (http://tis-div-rp-cerf.web.cern.ch/tis-div-rp-cerf).

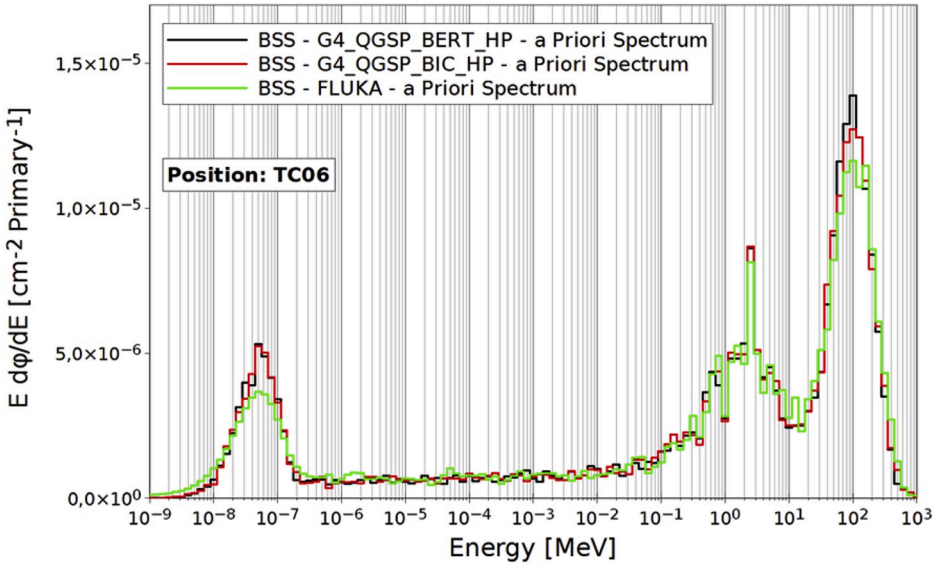

Fig. 6. Neutron energy spectra for pos. 6 on top of the concrete roof (TC06), measured with the ERBSS system; BSS - G4_QGSP_BERT_HP: the neutron energy spectrum simulated with GEANT4 and the Bertini physics list was used as a starting guess spectrum in the unfolding process; BSS – G4_QGSP_BIC_HP: the Binary physics list was used (Fig. 3); BSS-FLUKA: the re-binned FLUKA reference spectrum (http://tis-div-rp-cerf.web.cern.ch/tis-div-rp-cerf) was used (Fig. 3).

results obtained for the other reference positions are shown in the Appendix (Fig. A1-A3).

As for the simulated neutron energy spectra in Figs. 2 and 3, all results shown in Figs. 6 and 7 are normalized to one primary event. It is evident from Figs. 6 and 7 that the simulated neutron energy spectra do not depend much on the choice of the starting guess spectra (which is in line with what is reported in Simmer et al. (2010)), although in the case of the iron roof, the results obtained when using the FLUKA reference spectrum as a starting guess spectrum are somewhat lower than those obtained using the GEANT4 simulated spectra.

4. Discussion

In the following, the measured ERBSS neutron energy spectra are compared with the spectra obtained by MC simulations (Geant4, FLUKA). It should be noted, however, that some parameters that might influence the neutron spectra at the experimental site are not sufficiently known (for example the elemental composition of concrete, and in particular its water content). To investigate the influence of the water content of concrete, Duckic and Hayes (2018) simulated 14 MeV neutrons impinging perpendicularly on a concrete slab of 75 cm thickness (similar to the CERF facility where the concrete wall had a thickness of 80 cm). In their simulation (which was performed with MCNP) they used a somewhat different elemental composition for concrete as was used in the present study, but varied the mass fraction of water in the concrete. These authors showed that in such conditions, the neutron transmission factor was 9.39×10^{-2} (Sv cm^2 10^{10}) while it was 4.94×10^{-2} (Sv cm^2 10^{10}) for a water content of 9% and 2.5%, respectively. These results demonstrate the influence of the water content in concrete and, therefore, it should be kept in mind below where the results of the present GEANT4 simulations are compared to measurements that this parameter was not known. Any differences between simulation and measurement

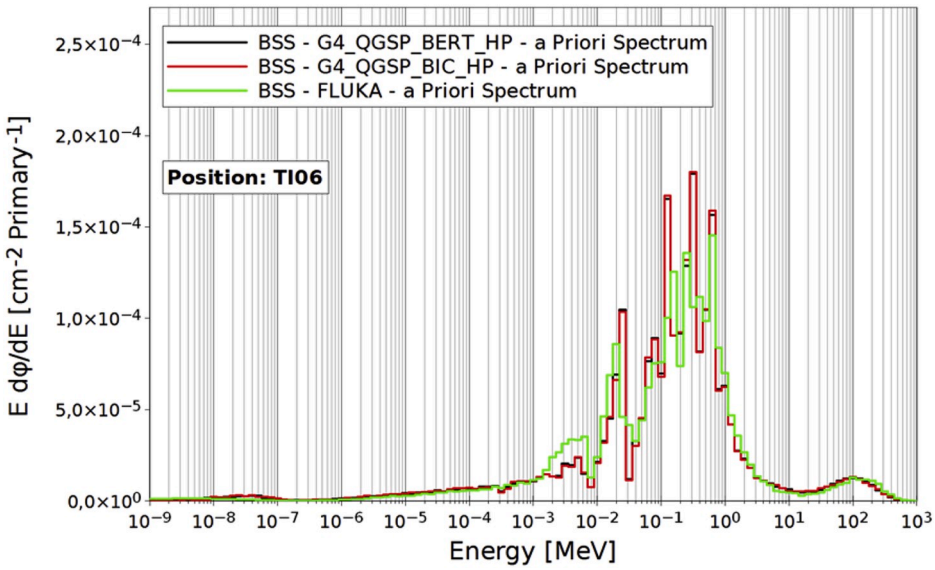

Fig. 7. Neutron energy spectra for pos. 6 on top of the iron roof (TI06), measured with the ERBSS system; BSS – G4_QGSP_BERT_HP: the neutron energy spectrum simulated with GEANT4 and the Bertini physics list was used (see Fig. 4) as a starting guess spectrum in the unfolding process; BSS – G4_QGSP_BIC_HP: the Binary physics list was used (Fig. 4); BSS-FLUKA: the re-binned FLUKA reference spectrum (http://tis-div-rp-cerf.web.cern.ch/tis-div-rp-cerf) was used (Fig. 4).

might thus be due to the unknown water content in concrete.

There are indications that the elemental composition and density for GG20 and S235 reported in Agosteo et al. (2013) might have been mixed. To verify the influence of iron densities on neutron fluence outside the iron wall, we performed simulations with the QGSP_BIC_HP physics list, calculated one million primary protons and compared the result with that obtained with the unchanged iron density. Depending on the measurement position, the total neutron fluence outside the iron wall was higher by 1.3–3.4%, for the changed iron density. This suggests that the iron density is not critical.

4.1. Discussion of total fluence

4.1.1. Comparison between simulated GEANT4 and FLUKA total neutron fluences

A qualitative comparison of the simulated neutron energy spectra (Figs. 3 and 4 for positions TC06 and TI06, respectively) suggests a rather good agreement, although some differences are notable (the same is true for the results simulated at the other reference positions – see Appendix). For a more quantitative analysis, the total neutron fluence simulated for each position with GEANT4 using either the Bertini or Binary physics list were normalized to the corresponding neutron fluence obtained from the FLUKA simulations (CERF reference spectra). It turned out that for all positions where FLUKA results were available (all positions (eight) except for the concrete side walls) the GEANT4 simulations using the Binary physics list were much closer to the FLUKA fluences than those obtained with the GEANT4 Bertini physics list. More specifically, when the neutron fluences obtained with GEANT4 were normalized to those obtained with FLUKA (Table A1) the mean ratio between Geant4 Binary and FLUKA was 1.13 ± 0.14, whereas that between Geant4 Bertini and FLUKA was 1.53 ± 0.14 (mean ± standard deviation of eight values). This result did not change much if data are restricted to concrete or iron separately. The difference between Geant4 Bertini and Binary is significant, as the statistical uncertainty involved in the Geant4 simulations was of the order of 2–3%, for total neutron fluence. As a matter of caution it should be noted, however, that comparison of the Geant4 and FLUKA simulations implies comparison of the complete MC models used (including for example CERF geometry, shielding materials, etc.) and not only comparison of the nuclear models used in these simulations. It should be also emphasized that the results obtained do not allow for any decision as to which physics list or MC code provides more correct results (even though the Geant4 Binary results were close to those obtained with FLUKA).

4.1.2. Comparison between simulated and measured total neutron fluences

At first glance, comparison of the simulated neutron fluences with those obtained based on the ERBSS measurements might provide a solution to this problem (e.g., comparison between Bertini and Binary GEANT4). In this respect it looks encouraging that the experimental neutron energy spectra unfolded from the ERBSS raw data do not depend on which of the MC codes and physics lists were used to simulate the start neutron spectrum required to initiate the unfolding process (Figs. 5 and 6). It should be kept in mind, however, that all experimental results obtained with the ERBSS were normalized to one incoming primary particle. Normalization was done based on the counts of a precision ionization chamber (PIC), where one count of this PIC, "PIC-cnt", is equivalent to 22,000 primary particles involving an uncertainty of ± 10% (Ferrari et al., 2014). Furthermore, quantitative ERBSS measurements require the knowledge of the response functions of all Bonner Spheres used in the spectrometer, for the whole range of neutron energies of interest. Those response functions cannot be measured for all energies but have to be simulated (again) with MC codes including the uncertainties involved in the choice of nuclear models used in these simulations. This issue was investigated in detail by Pioch et al. for the ERBSS system also used in the present work (Pioch et al., 2010), based on measurements of secondary neutrons from cosmic radiation at the Environmental Research Station UFS on the Zugspitze mountain, Germany (Leuthold et al., 2007). While the choice of nuclear models for simulation of ERBSS response functions is not critical for neutron energies below 20 MeV, where validated neutron interaction cross section data exist, for higher neutron energies use of the MCNP/LAHET approach results in response functions that lie typically between those calculated with GEANT4 BIC and GEANT4 Bert (Pioch et al., 2010). Pioch and co-workers came to the conclusion that "doses from secondary neutrons from cosmic radiation as deduced from ERBSS measurements are uncertain by about 10%, simply because of some differences in nuclear models used by various neutron transport codes." (Pioch et al., 2010). For total neutron fluence their results suggest somewhat smaller uncertainties (less than 5%), in part because larger uncertainties observed for fluences of epithermal and high-energy neutrons (which

were 13 and 18%, respectively) cancelled out. It should be mentioned that these results were obtained for the neutron energy spectrum of secondary neutrons from cosmic radiation, and it may well be that somewhat other uncertainties apply for other shapes of neutron energy spectra. It is therefore believed that a 5% uncertainty for total neutron fluence obtained in the present study might be too low, and an uncertainty of 10% was assumed instead.

Based on the above, an overall uncertainty in measured total neutron fluences of about 14% was assumed (10% from the PIC factor, and about 10% from the uncertain ERBSS response functions), and ratios were calculated for the total fluence simulated with GEANT4 and FLUKA and normalized to the corresponding mean values from the ERBSS measurements (including a statistical uncertainty of 3% for the simulated total neutron fluence). To give an example, for concrete roof, pos. 6 (TC06), the neutron energy spectra shown in Fig. 3 for the GEANT (Binary) simulation gave a total neutron fluence of 5.28×10^{-5} neutrons per cm^2 and primary particle (Table A1 in the Annex). The corresponding measured ERBSS neutron energy spectra shown in Fig. 5 gave 6.20×10^{-5}, 6.22×10^{-5}, and 6.13×10^{-5} neutrons per cm^2 and primary particle for BSS-BIC, BSS-BERT, and BSS-FLUKA, respectively, with a mean of 6.20×10^{-5} neutrons per cm^2 and primary particle (Table A1). Thus the normalized GEANT (Binary) value was $5.28 \times 10^{-5}/6.20 \times 10^{-5} = 0.85 \pm 0.13$ (where the uncertainty corresponds to 15%). This means that for total neutron fluence at position TC06, the GEANT4 (Binary) simulation gave (86 ± 13%) of the measured total neutron fluence. This kind of analysis was done for all reference positions on concrete roof, concrete side wall, and iron roof. The results for total neutron fluence are shown in Table 2 and graphically presented in Fig. 8.

The point estimates shown in Table 2 and Fig. 8 lie between +1.27 and – 0.6, indicating rather good agreement between simulations and measurements, whatever position, material, MC code and nuclear models considered. As a general trend, data simulated with GEANT4 Bertini appear to be closer to the measurements (i.e., the corresponding ratios are closer to 1) than those simulated with GEANT4 Binary or FLUKA. To be more specific, mean values and standard deviations were 0.77 ± 0.12, 1.06 ± 0.15, and 0.71 ± 0.07, for GEANT4 Binary, GEANT4 Bertini, and FLUKA, respectively. Results were similar if the data for top of concrete and top of iron were evaluated separately (note that for side of concrete, no FLUKA simulations were available, and the ERBSS measurements had to be performed with a subset of only six spheres): 0.76 ± 0.12, 1.08 ± 0.17, and 0.75 ± 0.05 for concrete, and 0.78 ± 0.10, 1.02 ± 0.11, and 0.66 ± 0.05 for iron, respectively (Table 3).

The results indicate that simulations with GEANT4 Bertini were somewhat closer to the ERBSS measurement results than those obtained with GEANT4 Binary or FLUKA, regardless which material was used as shielding material.

Table 2
Results of simulated total neutron fluence and H*(10) values, for the investigated reference positions, normalized to mean of corresponding ERBSS measured total fluence and H*(10) values.

Position/ MC-Code	Simulated total fluence Φ normalized to ERBSS measurement	Simulated total H*(10) normalized to ERBSS measurement
TC04		
Geant4 - BIC	0.92 ± 0.14	0.93 ± 0.14
Geant4 - BERT	1.27 ± 0.19	1.29 ± 0.19
FLUKA	0.79 ± 0.12	0.81 ± 0.13
TC06		
Geant4 - BIC	0.86 ± 0.13	0.87 ± 0.13
Geant4 - BERT	1.20 ± 0.18	1.19 ± 0.18
FLUKA	0.75 ± 0.11	0.84 ± 0.13
TC13		
Geant4 - BIC	0.83 ± 0.12	0.88 ± 0.13
Geant4 - BERT	1.20 ± 0.18	1.25 ± 0.19
FLUKA	0.79 ± 0.12	0.88 ± 0.13
TC15		
Geant4 - BIC	0.67 ± 0.10	0.78 ± 0.12
Geant4 - BERT	0.93 ± 0.14	1.06 ± 0.16
FLUKA	0.68 ± 0.10	0.75 ± 0.11
SC02		
Geant4 - BIC	0.73 ± 0.11	0.65 ± 0.10
Geant4 - BERT	1.05 ± 0.16	0.92 ± 0.14
SC04		
Geant4 - BIC	0.59 ± 0.09	0.52 ± 0.08
Geant4 - BERT	0.83 ± 0.12	0.70 ± 0.11
TI04		
Geant4 - BIC	0.92 ± 0.14	1.03 ± 0.15
Geant4 - BERT	1.16 ± 0.17	1.29 ± 0.19
FLUKA	0.67 ± 0.10	0.83 ± 0.12
TI06		
Geant4 - BIC	0.84 ± 0.13	0.94 ± 0.14
Geant4 - BERT	1.11 ± 0.17	1.22 ± 0.18
FLUKA	0.71 ± 0.11	0.75 ± 0.11
TI13		
Geant4 - BIC	0.63 ± 0.09	0.74 ± 0.11
Geant4 - BERT	0.87 ± 0.13	1.02 ± 0.15
FLUKA	0.67 ± 0.10	0.72 ± 0.11
TI15		
Geant4 - BIC	0.72 ± 0.11	0.85 ± 0.13
Geant4 - BERT	0.95 ± 0.14	1.12 ± 0.17
FLUKA	0.61 ± 0.09	0.64 ± 0.10

4.2. Discussion of total ambient dose equivalent (H*(10))

4.2.1. Comparison between simulated GEANT4 and FLUKA total H*(10) values

A similar evaluation of the data as that for total neutron fluence (see above) was also performed in terms of ambient dose equivalent (H*(10)).

To calculate ambient dose equivalent, the present neutron energy spectra simulated with GEANT4 and measured with the ERBSS were folded up to a neutron energy of 19 MeV with fluence to ambient dose equivalent conversion coefficients recommended by the International Commission on Radiological Protection (ICRP 74, 1997), extended beyond 19 MeV by those from Pellicioni (2000). The resulting ambient neutron dose equivalent values per primary particle for all investigated reference positions are shown in the last column of Table A1 in the Annex. When dose contributions were calculated separately for the four investigated energy intervals it turned out that for concrete, about half of the total dose was from neutrons with energies between 100 keV and 20 MeV, while the other half of the total dose was from neutrons with energies above 20 MeV. Neutrons with energies of less than 100 keV contributed only a few percent to total ambient dose equivalent (see also Prokopovich et al. (2010)).

In contrast, for iron between 90 and 95% of total ambient dose equivalent was from neutrons in the energy range between 100 keV and 20 MeV, while neutrons with energies above 20 MeV contributed only between 5 and 10% (data not shown). These results are also consistent with those reported by Pozzi et al. for the CERF facility, although these authors used slightly different measurement positions and energy ranges (Pozzi et al., 2019).

For a more quantitative comparison, the total H*(10) values simulated for each position with GEANT4 using either the Binary or Bertini physics list were normalized to the corresponding total H*(10) values obtained from the FLUKA simulations (CERF reference spectra). It turned out that for all positions where FLUKA results were available (all positions (eight) except for the concrete side walls) the GEANT4 simulations using the Binary physics list were much closer to the FLUKA total H*(10) values than those obtained with the GEANT4 Bertini physics list.

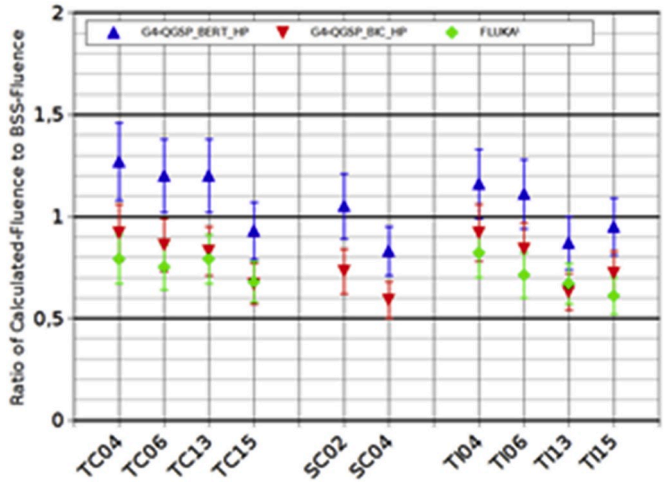

Fig. 8. Ratio of total neutron fluence simulated with Geant4 (QGSP_BIC_HP), Geant4 (QGSP_BERT_HP) and FLUKA reference values, each normalized to corresponding mean measured total neutron fluence values (ERBSS). Error bars include 15% overall uncertainty. Statistical uncertainties of the GEANT4 simulations were less than 3%.

Table 3
Total simulated neutron fluences relative to corresponding mean measured total neutron fluence for concrete + iron positions, concrete positions, and iron positions (data taken from Table 2); means ± one standard deviation.

Total neutron fluence	Geant4 BIC	Geant4 BERT	FLUKA
Concrete + Iron	0.77 ± 0.12	1.06 ± 0.15	0.71 ± 0.07
Concrete	0.76 ± 0.12	1.08 ± 0.17	0.75 ± 0.05
Iron	0.78 ± 0.10	1.02 ± 0.11	0.66 ± 0.05

More specifically, when the total H*(10) values obtained with GEANT4 were normalized to those obtained with FLUKA (Table A1) the mean ratio between Geant4 Binary and FLUKA was 1.12 ± 0.13, while that between Geant4 Bertini and FLUKA was 1.51 ± 0.13 (mean ± standard deviation of eight values). The results are very similar to those obtained for total neutron fluence (see above). The result also did not change much if data were restricted to concrete or iron separately. As for total neutron fluence, the difference between Geant4 Bertini and Binary is significant, as the statistical uncertainty involved in the Geant4 simulations was only of the order of 2–3%. As a matter of caution it should be emphasized again, however, that comparison of the Geant4 and FLUKA simulations implies comparison of the complete MC models used (including for example CERF geometry, shielding materials, etc.) and not only comparison of nuclear models used.

4.2.2. *Comparison between simulated and measured total H*(10) values*

The last column of Table 2 shows total simulated versus measured H*(10) values as calculated with Geant4 (Binary), Geant4 (Bertini), and FLUKA. Similar to the total neutron fluence values, means and standard deviations were then calculated for total H*(10) values for all positions, and for the concrete and iron positions separately (Table 4).

Again, Geant4 (Binary) results were somewhat closer to the measurements for the iron positions, while Geant4 (Bertini) were somewhat closer for the concrete positions, although the differences were not large (about 30% maximum). It is also evident that the FLUKA ambient neutron dose values were always lower than the corresponding means of the measured values although, again, the differences were not very large (about 27% maximum).

Table 4
Total simulated H*(10) values relative to corresponding mean measured H*(10) values for concrete + iron positions, concrete positions, and iron positions (data taken from Table 2); means ± one standard deviation.

H*(10) total	Geant4 BIC	Geant4 BERT	FLUKA
Concrete + Iron	0.82 ± 0.15	1.11 ± 0.19	0.79 ± 0.09
Concrete	0.77 ± 0.16	1.07 ± 0.22	0.84 ± 0.07
Iron	0.89 ± 0.12	1.16 ± 0.11	0.73 ± 0.08

4.2.3. *Comparison with H*(10) results published in the literature*

In a recent paper, Dinar et al. reported on an instrument intercomparison in the high-energy field at the CERF facility and compared the results they obtained at various reference positions with new FLUKA simulations (Dinar et al., 2018). In terms of ambient dose equivalent (H*(10)) given in nSv per count measured in a precision ionization chamber (PIC), comparison of their results with ours is directly possible for positions CT4, CT13, CT15, CS4, IT4 and IT13. Note again that one PIC count corresponds to 22,000 ± 10% primary particles. Additionally, their experimental result of an ERBSS measurement at position CS4 can also be compared with our results (Table 5).

From Table 5 it appears that for the concrete positions (TC04, TC13, TC15, and SC04) the new FLUKA values given by Dinar and co-workers are very close to but slightly lower than those of the older FLUKA reference values. In contrast, the new FLUKA values of Dinar et al. are somewhat higher than the older FLUKA reference values for the iron positions (TI04, TI13), although this difference is again not significant. For position SC04 Dinar and co-workers performed some measurements with a Bonner Sphere Spectrometer and obtained an H*(10) value of 0.343 ± 0.041 pSv per PIC-count. For the experimental uncertainty, the "BSS uncertainty is estimated at 12%. The sensitivity analysis and uncertainty propagation calculation were based on the statistical counting uncertainties (1%), the uncertainty on the number of delivered particles (10%), the uncertainty on the response matrix (3%) and the positioning uncertainty (3%)" (Dinar et al., 2018). To calculate H*(10) from their BSS neutron energy spectra, these authors used ICRP 74 fluence-to-H*(10) conversion coefficients (ICRP 74, 1997). The value of 0.40 ± 0.06 obtained in the present study with the ERBSS is consistent with the result reported by Dinar and co-workers.

5. Conclusion

In terms of the total neutron fluence measured with the ERBSS the Geant4 simulations with the "QGSP_BERT_HP" physics list performed

Table 5
Total neutron ambient dose equivalent (H*(10)) in pSv per count in a precision ionization chamber PIC (one PIC count corresponds to 22,000 ± 2200 incoming primary particles). CT – concrete top; CS – concrete side; IT – iron top. Last two columns: uncertainties as given by Dinar et al., (2018); Geant4 uncertainties: 3% from statistics and 10% from PIC factor; ERBSS uncertainties: 15% (10% from uncertainty in ERBSS response matrix and 10% from PIC factor); FLUKA uncertainties: 10% from PIC factor. [1]Data are from (http://tis-div-rp-cerf.web.cern.ch/tis-div-rp-cerf).

Reference position	Geant4 BIC, this work	GEANT4 Bertini, this work	FLUKA[1]	ERBSS, this work	FLUKA (Dinar et al., 2018)	BSS (Dinar et al., 2018)
TC4	0.21 ± 0.02	0.29 ± 0.3	0.20 ± 0.02	0.22 ± 0.03	0.185 ± 0.019	
TC13	0.22 ± 0.02	0.31 ± 0.03	0.22 ± 0.02	0.25 ± 0.04	0.203 ± 0.020	
TC15	0.23 ± 0.02	0.31 ± 0.03	0.22 ± 0.02	0.29 ± 0.04	0.217 ± 0.022	
SC04	0.21 ± 0.02	0.28 ± 0.03	–	0.40 ± 0.06	0.296 ± 0.030	0.343 ± 0.041
TI04	1.81 ± 0.18	2.27 ± 0.23	1.46 ± 0.20	1.76 ± 0.25	1.604 ± 0.161	
TI13	0.79 ± 0.08	1.09 ± 0.11	0.76 ± 0.11	1.06 ± 0.15	1.132 ± 0.113	

slightly better than those with the "QGSP_BIC_HP" physics list. While the simulations using the Bertini model tended to overestimate the measured fluences slightly (ratio of measured to simulated total neutron fluence of 1.02 ± 0.11 for iron and 1.08 ± 0.17 for concrete shielding) the Binary model tended to underestimate the measurements (ratio measured to simulated total neutron fluence of 0.78 ± 0.10 for iron and 0.76 ± 0.12 for concrete shielding). This tendency was observed for all neutron energies greater than 0.4 eV.

As compared to the measured values, total neutron fluences obtained by the FLUKA were similar to those obtained with Geant4 and both physics lists, for high energies (E > 20 MeV). In contrast, for the energy range between 0.4 eV and 20 MeV, the agreement became worse. More specifically, the total neutron fluence obtained by FLUKA was smaller than that measured, with a similar trend like the Geant4 Binary model (ratio of measured to FLUKA simulated total neutron fluences of 0.66 ± 0.05 for iron and 0.75 ± 0.05 for concrete shielding).

Similar trends were observed in terms of the neutron ambient dose equivalent (H*(10)). Additionally, for H*(10) behind the concrete shielding the Bertini model resulted in values which were slightly closer to those measured than those provided by the Binary model. In contrast, behind the iron shielding, the values obtained with the Binary model gave the best agreement with those measured.

Overall it is concluded that both, in terms of total neutron fluence and neutron ambient dose equivalent, the results obtained with Geant4 using the Bertini physics list were somewhat closer to the measurements, although the differences between the Bertini, Binary and FLUKA results were in a similar range. Consequently, no clear favorite of the two tested physics lists (Bertini or Binary), for the neutron field calculation at CERF, could be identified. It may also be concluded that the Bertini model might provide the most conservative (i.e., highest) dose estimate. In these discussions one should keep in mind, however, that by comparing the performance and outcome of the Geant4 and FLUKA simulations, one compares implicitly also the geometric models and shielding materials implemented in the two codes.

In the present study, measurements were performed at CERF at positions for which no experimental neutron spectra were publically available before. The results obtained suggest no major difference between the GEANT4 simulations and the ERBSS measurements performed. Moreover, results of the present GEANT4 simulations are in line with to those reference spectra obtained earlier by FLUKA.

Because the exact elemental composition of concrete at CERF (e. g. water content) was not exactly known and because there were some open issues on the iron density of the CERF iron wall, the results obtained in the present study and their comparison with measurements and other simulations must be interpreted with care. However, because our simulations are consistent with our ERBSS measurements, it appears that the water content of concrete at CERF is close to 9% as used in Geant4 simulations. For a systematical benchmark study, the elemental composition of the CERF materials must be known or a dedicated sensitivity analysis of the influence of the material composition must be performed.

Declaration of competing interest

The authors declare that they have no known competing financial interests or personal relationships that could have appeared to influence the work reported in this paper.

Acknowledgement

We would like to thank the staff of the CERF facility, for the opportunity to carry out this measurement campaign, and the support during the beam time.

This research received funding from the Bavarian State Ministry of the Environment and Consumer Protection, within the research project "Virtual Alpine Observatory" under contract number "71_1d-U8729-2013/193-5".

Appendix

Table A1
Results of simulated neutron fluence and H*(10) values per primary particle, for various energy ranges and reference positions using the Binary physics list ("Geant4-BIC), the Bertini physics list ("Geant4-Bert"), and the FLUKA reference values (taken from (http://tis-div-rp-cerf.web.cern.ch/tis-div-rp-cerf)); "BSS" - mean of corresponding measured neutron fluence values; Note that two energy intervals were combined for the positions on the iron roof, to account for the shape of the neutron fluence energy spectra simulated and measured there (Fig. A1 and A2).

Fluence Φ [cm^{-2}·Pri^{-1}]	E < 0.4 eV	0.4eV < E < 100 keV	100 keV < E < 20 MeV	E > 20 MeV	Total Fluence Φ [cm^{-2}·Pri^{-1}]	Total H*(10) [pSv·Pri^{-1}]
Concrete top, Pos. 4						
Geant4-BIC	8.398E-06	4.261E-06	1.033E-05	1.502E-05	3.800E-05	9.505E-03
GEANT4-Bert	1.155E-05	6.182E-06	1.484E-05	1.999E-05	5.255E-05	1.310E-02
FLUKA	4.722E-06	3.975E-06	9.562E-06	1.427E-05	3.253E-05	9.085E-03
BSS	6.615E-06	6.838E-06	1.261E-05	1.532E-05	4.138E-05	1.019E-02
Concrete top, Pos. 6						
Geant4-BIC	1.073E-05	6.034E-06	1.430E-05	2.177E-05	5.283E-05	1.330E-02
GEANT4-Bert	1.579E-05	9.263E-06	2.074E-05	2.844E-05	7.423E-05	1.830E-02
FLUKA	6.631E-06	5.775E-06	1.368E-05	2.058E-05	4.667E-05	1.285E-02
BSS	9.300E-06	9.600E-06	1.900E-05	2.400E-05	6.200E-05	1.538E-02
Concrete top, Pos. 13						
Geant4-BIC	8.350E-06	4.835E-06	1.090E-05	1.653E-05	4.062E-05	1.002E-02
GEANT4-Bert	1.243E-05	7.587E-06	1.654E-05	2.218E-05	5.874E-05	1.428E-02
FLUKA	6.258E-06	5.416E-06	1.102E-05	1.622E-05	3.892E-05	1.008E-02
BSS	8.200E-06	8.600E-06	1.500E-05	1.700E-05	4.900E-05	1.140E-02
Concrete top, Pos. 15						
Geant4-BIC	7.857E-06	4.475E-06	1.075E-05	1.729E-05	4.037E-05	1.036E-02
GEANT4-Bert	1.104E-05	6.562E-06	1.573E-05	2.224E-05	5.557E-05	1.412E-02
FLUKA	8.190E-06	5.768E-06	1.065E-05	1.589E-05	4.050E-05	9.887E-03
BSS	1.200E-05	1.100E-05	1.800E-05	1.900E-05	6.000E-05	1.328E-02
Concrete side, Pos. 2						
Geant4-BIC	2.418E-05	1.149E-05	1.800E-05	1.900E-05	7.213E-05	1.361E-02
GEANT4-Bert	3.532E-05	1.719E-05	2.700E-05	2.500E-05	1.039E-04	1.940E-02

(*continued on next page*)

Table A1 (*continued*)

Fluence Φ [cm^{-2}·Pri^{-1}]	E < 0.4 eV	0.4eV < E < 100 keV	100 keV < E < 20 MeV	E > 20 MeV	Total Fluence Φ [cm^{-2}·Pri^{-1}]	Total H*(10) [pSv·Pri^{-1}]
BSS	2.409E-05	1.694E-05	2.766E-05	3.058E-05	9.927E-05	2.107E-02
Concrete side, Pos. 4						
Geant4-BIC	1.919E-05	8.094E-06	1.300E-05	1.200E-05	5.217E-05	9.433E-03
GEANT4-Bert	2.742E-05	1.272E-05	1.800E-05	1.500E-05	7.366E-05	1.289E-02
BSS	2.445E-05	1.464E-05	2.551E-05	2.380E-05	8.841E-05	1.829E-02
	E < 0.4 eV	0.4eV < E < 20 MeV		E > 20 MeV	Total	**Total H*(10)**
Iron top, Pos. 4						
Geant4-BIC	1.279E-06	4.204E-04		1.259E-05	4.343E-04	8.225E-02
GEANT4-Bert	1.659E-06	5.279E-04		1.773E-05	5.472E-04	1.032E-01
FLUKA	1.526E-06	3.013E-04		1.267E-05	3.155E-04	6.640E-02
BSS	6.700E-06	4.500E-04		1.000E-05	4.700E-04	7.986E-02
Iron top, Pos. 6						
Geant4-BIC	1.231E-06	4.316E-04		1.958E-05	4.524E-04	9.083E-02
GEANT4-Bert	1.624E-06	5.681E-04		2.683E-05	5.966E-04	1.183E-01
FLUKA	2.055E-06	3.611E-04		2.156E-05	3.847E-04	7.201E-02
BSS	6.700E-06	5.100E-04		2.600E-05	5.400E-04	9.669E-02
Iron top, Pos. 13						
Geant4-BIC	1.467E-06	1.706E-04		9.201E-06	1.813E-04	3.582E-02
GEANT4-Bert	2.015E-06	2.363E-04		1.329E-05	2.517E-04	4.932E-02
FLUKA	4.216E-06	1.760E-04		1.278E-05	1.929E-04	3.467E-02
BSS	7.600E-06	2.700E-04		1.500E-05	2.900E-04	4.830E-02
Iron top, Pos. 15						
Geant4-BIC	1.437E-06	3.385E-04		1.506E-05	3.549E-04	6.945E-02
GEANT4-Bert	1.752E-06	4.426E-04		2.042E-05	4.648E-04	9.117E-02
FLUKA	5.028E-06	2.788E-04		1.520E-05	2.990E-04	5.217E-02
BSS	1.100E-05	4.700E-04		1.400E-05	4.900E-04	8.141E-02

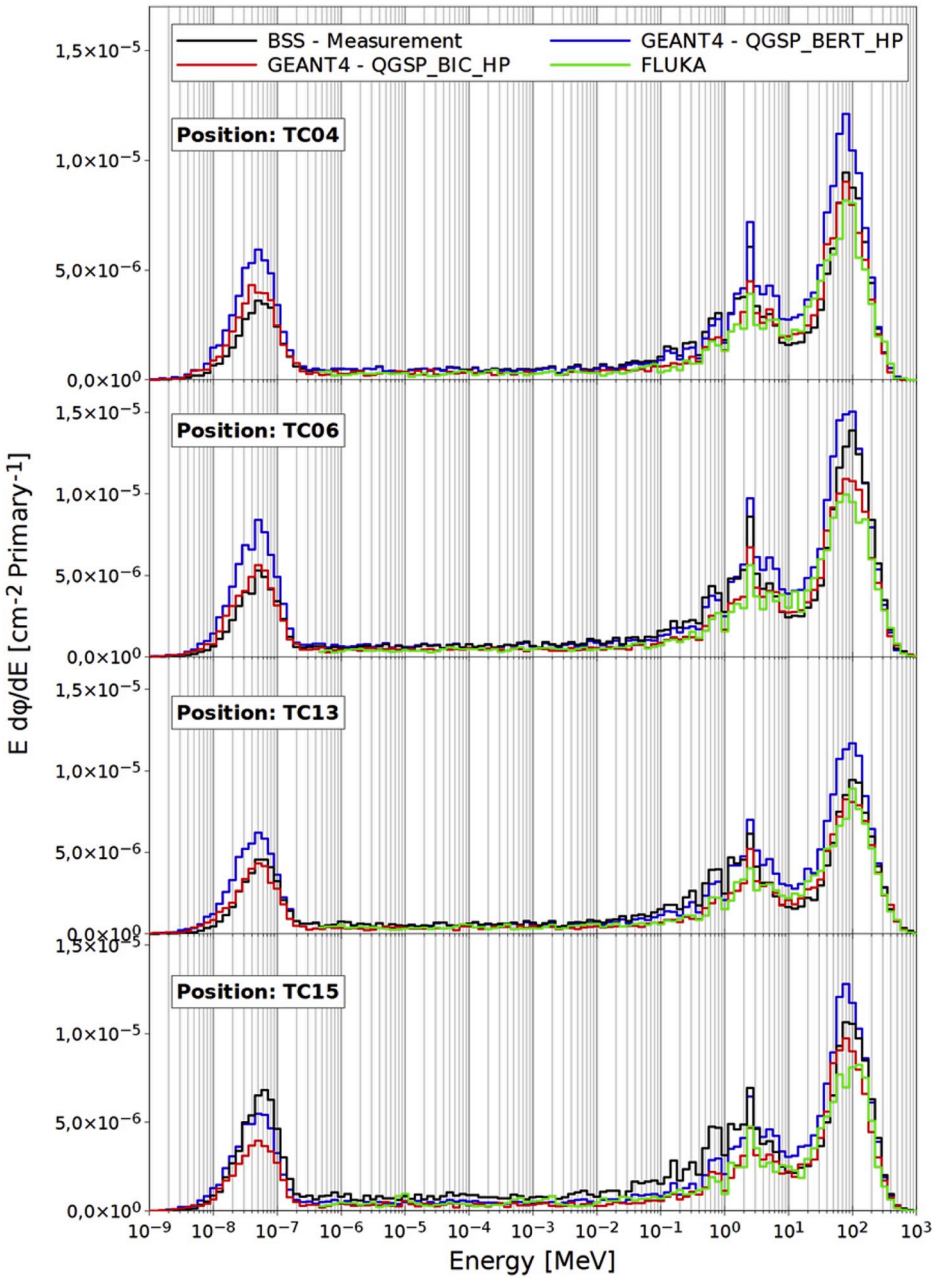

Fig. A1. Neutron energy spectra behind concrete top shielding on all four positions (TC04, TC06, TC13 and TC15). Black: BSS measurement, green: FLUKA reference value (http://tis-div-rp-cerf.web.cern.ch/tis-div-rp-cerf), blue and red: Geant4 with QGSP_BERT_HP and QGSP_BIC_HP as physics list.

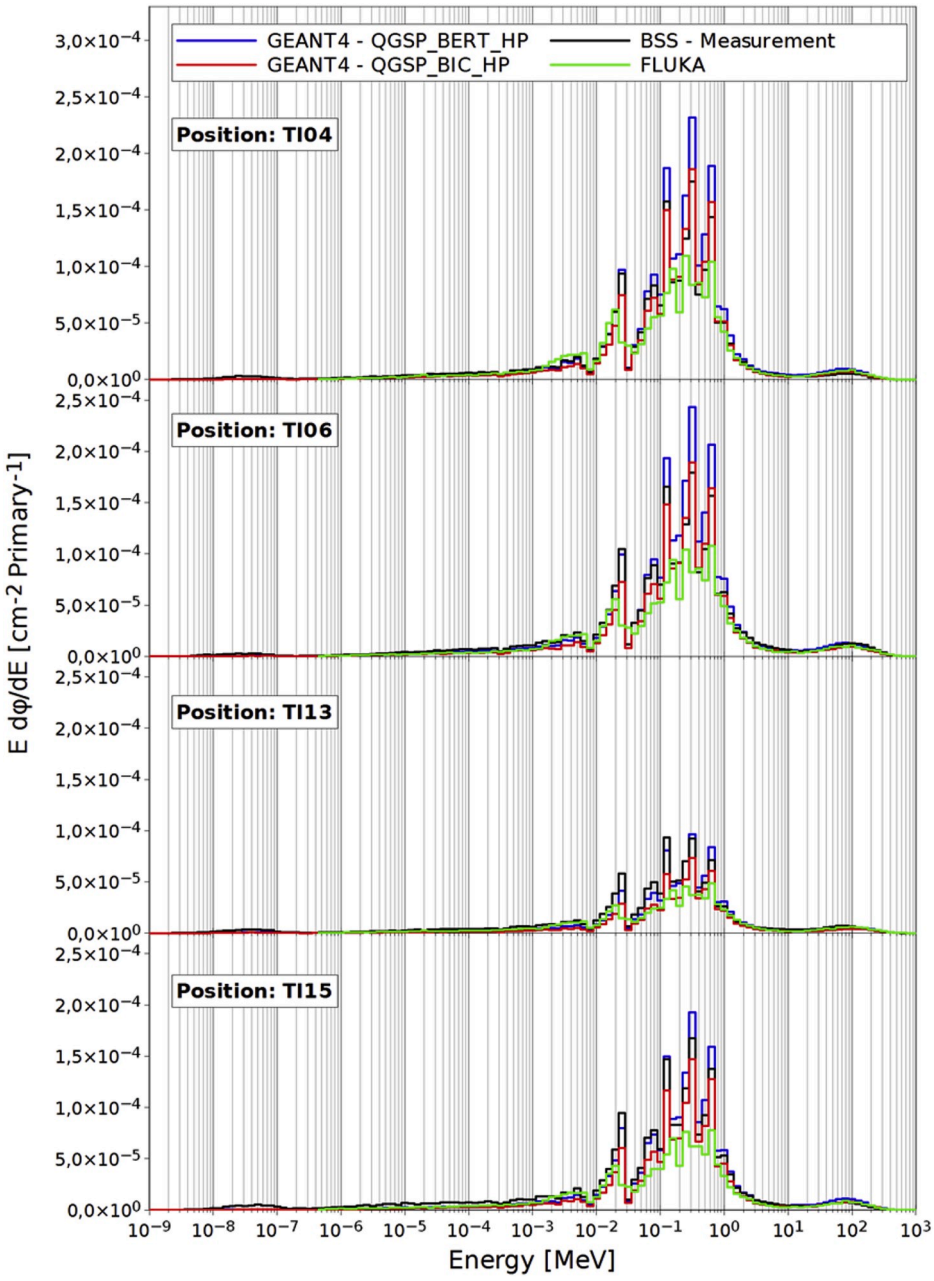

Fig. A2. Neutron energy spectra behind iron top shielding on all four positions (TI04, TI06, TI13 and TI15). Black: BSS measurement, green: FLUKA reference value (http://tis-div-rp-cerf.web.cern.ch/tis-div-rp-cerf), blue and red: Geant4 with QGSP_BERT_HP and QGSP_BIC_HP as physics list.

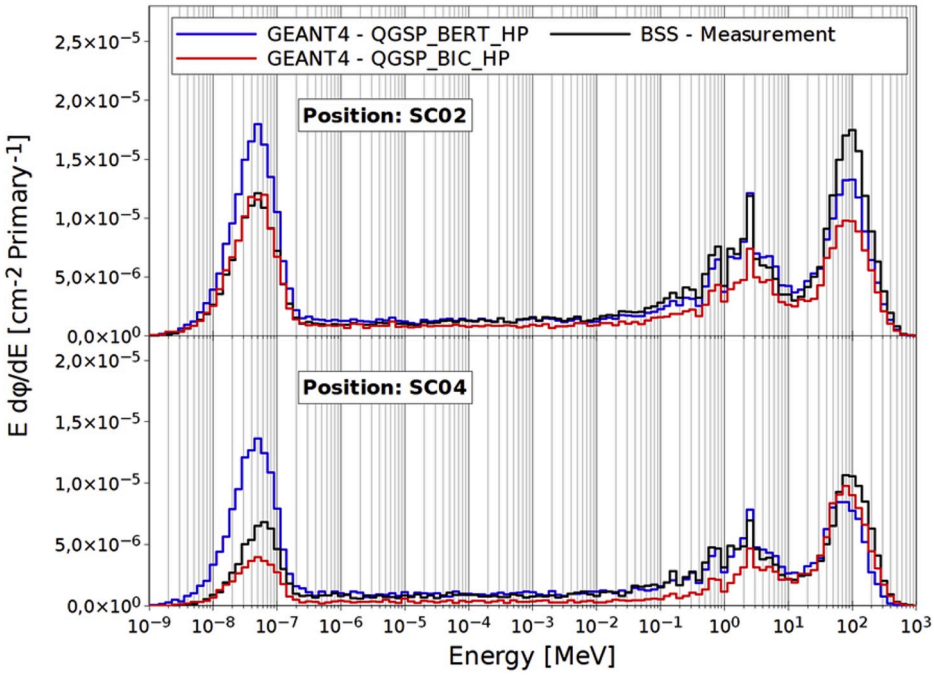

Fig. A3. Neutron energy spectra behind concrete side shielding on all four positions (SC02 and SC04). Black: BSS measurement, blue and red: Geant4 with QGSP_BERT_HP and QGSP_BIC_HP as physics list.

References

Agosteo, S., Pozzi, F., Silari, M., Ulrici, L., 2013. Attenuation in iron of neutrons produced by 120 GeV/c positive hadrons on a thick copper target. Nucl. Instrum. Methods Phys. Res., Sect. B 312, 36–41.

Agostinelli, S., 2003. Geant4 - a simulation toolkit. Nucl. Instrum. Methods Phys. Res., Sect. A 506, 250–303.

Alevra, A.V., Cosack, M., Hunt, J.B., Thomas, D.J., Schraube, H., 1992. Experimental determination of the response of four Bonner sphere sets to monoenergetic neutrons (II) Radiat. Prot. Dosim. 40, 91-10.

Alves, J., Bottollier-Depois, J.F., Fantuzzi, E., Fattibene, P., Lopez, M.A., Mayer, S., Miljanić, S., Olko, P., Rühm, W., Schuhmacher, H., Stadtmann, H., Vanhavere, F., 2015. Letter to the editor. Radiat. Protect. Dosim. 163, 268.

Aroua, A., Hofert, M., Sannikov, A.V., Stevenson, G.R., 1994. Reference High-Energy Radiation Fields at CERN. Report CERN/TIS-RP/94-12/CF. European Laboratory for Particle Physics.

Birattari, C., Rancati, T., Hoefert, M., Otto, T., Silari, M., 1998. Recent results at the CERN-EC high energy reference field facility. In: SATIF-3 Shielding Aspects of Accelerators, Targets and Irradiation Facilities: Tohoku University, Sendai, Japan 12-13 May 1997, Sendai, Japan, 12-13 May 1997, pp. 219–234.

Bramblett, R.L., Ewing, R.I., Bonner, T.W., 1960. A new type of neutron spectrometer. Nucl. Instrum. Methods Phys. Res. 9, 1–12.

Dinar, N., Pozzi, F., Silari, M., Puzo, P., Chiriotti, S., De Saint-Hubert, M., Vanhavere, F., Van Hoey, O., Orchard, G.M., Waker, A.J., 2018. Instrument intercomparison in the highenergy field at the CERN-EU Reference Field (CERF) facility and comparison with the 2017 FLUKA simulations. Radiat. Meas. 117, 24–34.

Duckic, P., Hayes, R.B., 2018. Total ambient dose equivalent buildup factor determination for NBS04 concrete. Health Phys. 114 (6), 569–581.

Fasso, A., Ferrari, A., Ranft, J., Sala, P.R., Stevenson, G.R., Zazula, J.M., 1993. FLUKA92. In: Proceedings of the Workshop on Simulating Accelerator Radiation Environments, Santa Fe, USA, pp. 11–15.

Ferrari, A., La Torre, F.P., Manessi, G.P., Pozzi, F., Silari, M., 2014. Monitoring reactions for the calibration of relativistic hadron beams. Nucl. Instrum. Methods Phys. Res., Sect. A 763, 177–183.

Geant4 Collaboration, 2014. Geant4 User's Guide for Aplication Developers, Version: 10.1. http://geant4-userdoc.web.cern.ch/geant4-userdoc/UsersGuides/ForApplicationDeveloper/BackupVersions/V10.1/html/index.html.

Geant4 Collaboration, 2017. Guide for physics lists release 10.4. http://geant4-userdoc.web.cern.ch/geant4-userdoc/UsersGuides/PhysicsListGuide/BackupVersions/V10.4/html/index.html.

Höfert, M., Stevenson, G.R., 1994. The CERN-CEC High-Energy Reference Field Facility. Report CERN/TIS-RP/94-02/CF. European Laboratory for Particle Physics.

ICRP International Commission on Radiological Protection, 1997. Conversion coefficients for use in radiological protection against external radiation. ICRP publication 74, oxford: pergamon ICRP, conversion coefficients for use in radiological protection against external radiation. Ann. ICRP 26 (3/4) (ICRP Publication 74).

Leuthold, G., Mares, V., Rühm, W., Weitzenegger, E., Paretzke, H.G., 2007. Long-term measurements of cosmic ray neutrons by means of a bonner spectrometer at mountain altitudes – first results. Radiat. Protect. Dosim. 126 (1–4), 506–511.

Mares, V., Schraube, H., 1998b. High energy neutron spectrometry with Bonner spheres. In: Proceedings, the IRPA Regional Symposium on Radiation Protection in Neighbouring Countries of Central Europe, Prague, Czech Republic, September 1997, pp. 543–547.

Mares, V., Schraube, G., Schraube, H., 1991. Calculated neutron response of a Bonner sphere spectrometer with ^{3}He counter. Nucl. Instrum. Methods A 307, 398–412.

Mares, V., Sannikov, A., Schraube, H., 1998. The response functions of a ^{3}He-Bonner spectrometer and their experimental verification in high energy neutron fields. In: Proceedings of the 3rd Specialist Meeting on Shielding Aspects of Accelerators Targets and Irradiation Facilities, Sendai, Japan, pp. 237–248.

Mares, V., Sannikov, A.V., Schraube, H., 2002. Response functions of the Andersson-Braun and extended range rem counters for neutron energies from thermal to 10 GeV. Nucl. Instrum. Methods Phys. Res., Sect. A 476, 341–346.

Mares, V., Pioch, C., Rühm, W., Iwase, H., Iwamoto, Y., Hagiwara, M., Satoh, D., Yashima, H., Itoga, T.*, Sato, T., Nakane, Y., Nakashima, H., Sakamoto, Y., Matsumoto, T., Masuda, A., Harano, H., Nishiyama, J., Theis, C., Feldbaumer, E., Jaegerhofer, L., Tamii, A., Hatanaka, K., Nakamura, T., 2013. Neutron dosimetry in quasi-monoenergetic fields of 244 and 387 MeV. IEEE Trans. Nucl. Sci. 60, 299–304.

Matzke, M., 1987. Private Communication Later Integrated into the Neutron Metrology File IAEA1279 ZZ-NMF-90 available from: NEA Databank. www.oecd-nea.org/tools/abstract/detail/iaea1279.

Mitaroff, A., Silari, M., 2002. The CERN-EU High-Energy Reference Field (CERF) facility for dosimetry at commercial flight altitudes and in space. Radiat. Protect. Dosim. 102 (1), 7–22.

Nakao, N., Rokni, S.H., Brugger, M., Roesler, S., Vincke, H., Kasoka, K., 2006. Calculations of high-energy neutron spectra with different Monte Carlo transport codes and comparison to experimental data obtained at the CERF facility. In: Proceedings of 8th Shielding Aspects of Accelerators, Targets and Irradiation Facilities (SATIF8), Pohang Accelerator Laboratory (PAL), Korea, 22-24 May 2006.

Nakao, N., Taniguchi, S., Roesler, S., Brugger, M., Hagiwara, M., Vincke, H., Khater, H., Prinz, A.A., Rokni, S.H., Kosako, K., 2008. Measurement and calculation of high-energy neutron spectra behind shielding at the CERF 120 GeV/c hadron beam facility. Nucl. Instrm. Methods B 266, 93–106.

Pelliccioni, M., 2000. Overview of fluence-to-effective dose and fluence-to-ambient dose equivalent conversion coefficients for high energy radiation calculated using the FLUKA code Radiat. Prot. Dosim. 88, 279–297.

Pioch, C., Mares, V., Rühm, W., 2010. Influence of Bonner sphere response functions above 20 MeV on unfolded neutron spectra and doses. Radiat. Meas. 45, 1263–1267.

Pomp, S., Bartlett, D.T., Mayer, S., Reitz, G., Röttger, S., Silari, M., Smit, F.D., Vincke, H., Yasuda, H., 2013. High-energy Quasi-Monoenergetic Neutron Fields: Existing Facilities and Future Needs. European Radiation Dosimetry Group, EURADOS Report 2013-02, Braunschweig, Germany.

Pozzi, F., Ferrarini, M., Ferrulli, F., Silari, M., 2019. Impact of the newly proposed ICRU/ICRP quantities on neutron calibration fields and extended range neutron rem-counters. J. Radiol. Prot. 39, 920–937.

Prokopovich, D.A., Reinhard, M.I., Cornelius, I.M., Rosenfel, A.B., 2010. Geant4 simulation of the CERN-EU High-Energy Reference Field (CERF) facility. Radiat. Protect. Dosim. 141 (2), 106–113.
Schraube, H., Mares, V., Roesler, S., Heinrich, W., 1999. Experimental verification and calculation of aviation route doses. Radiat. Protect. Dosim. 86 (No 4), 309–315.
Schuhmacher, H., 2004. Neutron calibration facilities. Radiat. Protect. Dosim. 110, 33–42.
Silari, M., Pozzi, F., 2017. The CERN-EU High-Energy Reference Field (CERF) facility: applications and latest developments. EPJ Web Conf. 153, 1–6, 0300.
Simmer, G., Mares, V., Weitzenegger, E., Rühm, W., 2010. Iterative unfolding for bonner sphere spectrometers using the MSANDB code - sensitivity analysis and dose calculation. Radiat. Meas. 45, 1–9.
Thomas, D.J., Alevra, A.V., Hunt, J.B., Schraube, H., 1994. Experimental determination of the response of four Bonner sphere sets to thermal neutrons Radiat. Prot. Dosim. 54, 25–31.
Wielunski, M., Schütz, R., Fantuzzi, E., Pagnamenta, A., Wahl, W., Palfalvi, J., Zombori, P., Andrasi, A., Stadtmann, H., Schmitzer, Ch, 2004. Study of the sensitivity of neutron sensors consisting of a converter plus Si charged-particle detector. Nucl. Instrum. Methods 517, 240–253. http://tis-div-rp-cerf.web.cern.ch/tis-div-rp-cerf.
Wielunski, M., Brall, T., Dommert, M., Trinkl, T., Rühm, W., Mares, V., 2018. Electronic neutron dosimeter in high-energy neutron fields. Radiat. Meas. 114, 12–18.